Occurrence, gas/particle partitioning and carcinogenic risk of polycyclic aromatic hydrocarbons and their oxygen and nitrogen containing derivatives in Xi'an, central China

Chong Wei [a,b,c,d], Yongming Han [a,c,*], Benjamin A. Musa Bandowe [b], Junji Cao [a,c,e], Ru-Jin Huang [a,f], Haiyan Ni [a,c,d], Jie Tian [a,c,d], Wolfgang Wilcke [b,g]

[a] Key Laboratory of Aerosol Chemistry & Physics (KLACP), Institute of Earth Environment, Chinese Academy of Sciences, Xi'an 710075, China
[b] Geographic Institute, University of Berne, Hallerstrasse 12, 3012 Berne, Switzerland
[c] State Key Laboratory of Loess and Quaternary Geology (SKLLQG), Institute of Earth Environment, Chinese Academy of Sciences, Xi'an 710075, China
[d] University of Chinese Academy of Sciences, Beijing 100049, China
[e] Institute of Global Environmental Change, Xi'an Jiaotong University, Xi'an 710049, China
[f] Laboratory of Atmospheric Chemistry, Paul Scherrer Institute, 5232 Villigen PSI, Switzerland
[g] Institute of Geography and Geoecology, Karlsruhe Institute of Technology (KIT), Reinhard-Baumeister-Platz 1, 76131 Karlsruhe, Germany

HIGHLIGHTS

- Gaseous and particulate PAHs, OPAHs, NPAHs and AZAs were measured at Xi'an.
- $\sum$29PAHs were 1 to 2 orders of magnitude higher than $\sum$15OPAHs, $\sum$11NPAHs and $\sum$4AZAs.
- MW can predict phase partitioning and more absorption occurred in September.
- Gaseous PACs contributed 29 − 44% of total cancer risk

ARTICLE INFO

ABSTRACT

29 parent- and alkyl-polycyclic aromatic hydrocarbons (PAHs), 15 oxygenated-PAHs (OPAHs), 11 nitrated-PAHs (NPAHs) and 4 azaarenes (AZAs) in both the gaseous and particulate phases, as well as the particulate-bound carbon fractions (organic carbon, elemental carbon, char, and soot) in ambient air sampled in March and September 2012 from an urban site in Xi'an, central China were extracted and analyzed. The average concentrations (gaseous + particulate) of $\sum$29PAHs, $\sum$15OPAHs, $\sum$11NPAHs and $\sum$4AZAs were 1267.0 ± 307.5, 113.8 ± 46.1, 11.8 ± 4.8 and 26.5 ± 11.8 ng m^{-3} in March and 784.7 ± 165.1, 67.2 ± 9.8, 9.0 ± 1.5 and 21.6 ± 5.1 ng m^{-3} in September, respectively. Concentrations of $\sum$29PAHs, $\sum$15OPAHs and $\sum$11NPAHs in particulates were significantly correlated with those of the carbon fractions (OC, EC, char and soot). Both absorption into organic matter in particles and adsorption onto the surface of particles were important for PAHs and OPAHs in both sampling periods, with more absorption occurring in September, while adsorption was always the most important process for NPAHs. The total carcinogenic risk of PAHs plus the NPAHs was higher in March. Gaseous compounds, which were not considered in most previous studies, contributed 29 to 44% of the total health risk in March and September, respectively.

1. Introduction

Polycyclic aromatic hydrocarbons (PAHs), a group of organic contaminants containing two or more benzene rings, are ubiquitous environmental pollutants worldwide. The oxygenated-PAHs (OPAHs) included in this study and nitrated-PAHs (NPAHs) are derivatives of

PAHs containing carbonyl- and nitro-functional groups, respectively (Atkinson and Arey, 1994; Lundstedt et al., 2007). Azaarenes (AZAs) are a group of heterocyclic PAHs containing one nitrogen atom in place of a carbon atom within the aromatic ring (Bleeker et al., 1999). These polycyclic aromatic compounds (PACs) are formed and released into the environment mainly from the incomplete combustion of fossil fuels and biomass (Albinet et al., 2007; Bleeker et al., 1999; Lima et al., 2005). There are also natural sources of AZAs (e.g., microbial mycotoxins and plant-produced alkaloids) (Bleeker et al., 1999) and parent-PAHs like naphthalene and perylene (Bandowe et al., 2009;

* Corresponding author at: 10 Fenghui South Road, High-Tech Zone, Xi'an 710075, China. Tel.: +86 29 88329320; fax: +86 29 88320456.
E-mail address: yongming@ieecas.cn (Y. Han).

Wilcke, 2007; Wilcke et al., 1999) in the environment. OPAHs and NPAHs can also be formed in the atmosphere by the direct photolysis of parent-PAHs or homogeneous and heterogeneous reactions between parent-PAHs and atmospheric oxidants (e.g., O_3, OH and NO_x) (Atkinson and Arey, 1994; Lundstedt et al., 2007; Huang et al., 2014).

Elemental carbon (EC, also referred to as black carbon) mainly originates from the incomplete combustion of biomass and fossil fuels and is also ubiquitous in the environment (Goldberg, 1985; Han et al., 2010). It can be subdivided into char and soot (Han et al., 2010). Char is a carbonaceous material formed by the pyrolysis of organic substances and is therefore contained in combustion residues of incomplete burning, while soot refers to carbon particles formed at high temperatures via gas-to-particle conversion processes (Han et al., 2010). On heating, the organic compounds are partially cracked to smaller and unstable fragments, which are reactive free radicals with a short lifetime. These fragments form more stable PACs through recombination reactions (Mastral and Callén, 2000). This formation process can also be referred to as a "waterfall mechanism", in which soot and other complex-structure compounds with high molecular weight are formed through the combination of small fragments during combustion (Mastral and Callén, 2000). Hence, to some extent, soot and PACs have similar sources and formation mechanisms, and high molecular weight PACs can be considered to be precursors of soot.

PACs can be released into ambient air and partitioned into both gaseous and particulate phases, with a large fraction of PACs present in part or almost exclusively in the gaseous phase (Klein et al., 2006). The partition process is relevant to their occurrence in the atmosphere, fate (deposition, stability and long-range transport), and toxicity (Harner and Bidleman, 1998; Ringuet et al., 2012; Schnelle-Kreis et al., 2007). The two main mechanisms of partition are adsorption onto the surface of particles and absorption into the organic matter in particles (Harner and Bidleman, 1998; Ringuet et al., 2012). The difference in the sorption mechanism of PAHs is usually studied by plotting their experimental gas-particulate partition coefficient (K_p) against the sub-cooled vapor pressure (P_L^0) to generate a linear equation, the slope of which is related to the sorption mechanism (Harner and Bidleman, 1998; Pankow, 1987, 1994a,b; Pankow and Bidleman, 1991; Ringuet et al., 2012). Usually a slope (m_r) < -1 indicates adsorption to a strong sorbent, and > -0.6 absorption to a medium with high cohesive energy, while an m_r between -1 and -0.6 indicates that both adsorption and absorption occurred (Pankow, 1987, 1994a,b; Pankow and Bidleman, 1991; Terzi and Samara, 2004). The intercept (b_r) of the regression line depends on properties associated with the particles (Pankow, 1994a; Pankow and Bidleman, 1992). Most previous studies have focused on parent-PAHs, whereas little is known about the phase partitioning of OPAHs, NPAHs and AZAs (Albinet et al., 2007, 2008; Bandowe et al., 2014; Wang et al., 2011a).

The United States Environmental Protection Agency (U.S. EPA) lists 16 parent-PAHs as priority pollutants because of their carcinogenic, mutagenic and teratogenic properties (Eisler, 1987). OPAHs, AZAs and NPAHs are recognized as direct/indirect acting mutagens and carcinogens that generate more toxic and estrogenic effects than their parent-PAHs (Albinet et al., 2008; Rosenkranz and Mermelstein, 1985). The toxic potency of individual PAHs can be assessed according to their benzo[a]pyrene equivalent concentration (BaP_{eq}), based on the concept established by Nisbet and LaGoy (1992). Toxicological assessments have been extensively investigated for PAHs bound to particles (Bandowe et al., 2014; Ramírez et al., 2011). Few studies have considered gaseous pollutants (Gaga et al., 2012; Klein et al., 2006), although they may pose more risk to human health than particle-bound compounds because they can more easily enter the blood system following uptake via breathing.

Xi'an is the capital city of Shaanxi Province and is a popular tourist destination in central China; however, it has experienced serious air pollution, especially by particulate matter (PM), in recent years (Cao et al., 2005; Han et al., 2010). Therefore, gaseous and particulate bound-PACs were collected at Xi'an in March and September 2012, to determine their occurrence, phase partitioning, and carcinogenic risk.

2. Materials and methods

2.1. Sampling

Gaseous and particulate samples were collected simultaneously in 28–30 March and 6–10 September 2012 at the sampling platform of the Institute of Earth Environment, Chinese Academy of Sciences (IEECAS), located in the southeastern part of downtown Xi'an in an area with a mixture of urban, industrial, commercial and traffic use (Xu et al., 2012) (Fig. S1, A, shown in the Supplementary information, SI). A total of seven samples were collected on continuous three and four days sampling in March and September, respectively. Particulate and gaseous phase samples were acquired using an assembled cartridge containing quartz microfiber filters (QM/A, diameter: 90 mm, Whatman, Maidstone, UK), followed by a glass polyurethane foam (PUF) holder containing PUF plugs (60 mm diameter × 75 mm length, Peta, Guangzhou, China) (Fig. S1, B). The system was connected to a pump to collect total suspended particle (TSP) and gaseous samples for 24 h (from 10:00 am to 10:00 am). This system was controlled by a flow meter installed before the pump that was used to maintain a flow of 30 L min^{-1}. The inlet flow was also measured using a digital display Defender-520 air-flow calibrator (Mesa Laboratories, Lakewood, CO, USA) at the beginning and end of sampling. The real flow was calculated using the average value of the beginning and end flow, while the final sampling volume was converted to standard conditions (0 °C, 1.01×10^{-5} Pa). Prior to sampling, all quartz fiber filters were baked at 780 °C for 4 h in a muffle furnace to remove any organic compounds that might be present on the filters. PUFs were pre-eluted with dichloromethane (DCM) using a Soxhlet Extraction System for 24 h. After collection, the filters were wrapped in pre-baked aluminum foil and stored at −20 °C, while the PUFs were also stored at −20 °C in their stainless steel containers.

The average temperature (T) was 19.5 °C during the September sampling period, which was higher than the March sampling period (13.9 °C) (Table S1). Wind speed (WS) was 1.4 m s^{-1} in September, which was comparable to that in March (1.3 m s^{-1}) (Table S1). The dominant wind directions were south-west (SW, 39%) and north-west (NW, 37%) in March and September, respectively (Fig. S2).

2.2. Analysis of carbon fractions and PACs

The mass of total suspended particles (TSP) was obtained by weighing the filters twice before and after sampling using an electronic microbalance with 0.1 mg sensitivity (LA130S-F, Sartorius, Göttingen, Germany) in a controlled temperature (20–25 °C) and relative humidity (35–45%) environment (Han et al., 2010). The filters were equilibrated for 24 h at constant temperature (22 °C) and humidity (17%) in an environment chamber (MC108F, MeRyOu, Wuppertal, Germany) before gravimetric analysis.

2.2.1. Carbon fractions

Four C pools, i.e., organic carbon (OC), elemental carbon (EC), char and soot, were determined using a Desert Research Institute (DRI) Model 2001 Carbon Analyzer (Atmoslytic Inc. Calabasas, CA, USA) following the IMPROVE TOR protocol, which is described elsewhere (Cao et al., 2004; Chow et al., 1993; Han et al., 2007). Char and soot were measured following the definition by Han et al. (2007), with their sum being EC.

2.2.2. PACs

Details of the method used for the analysis of PACs are described in the Supplementary information. Briefly, filters containing sampled particulate PACs and PUFs containing gaseous PACs were analyzed separately. Half of each filter and the whole of each PUF were cut into small pieces, placed in 33 mL Accelerated Solvent Extractor (ASE) extraction cells (Dionex, Sunnyvale, CA, USA), spiked with seven perdeuterated-PAHs (naphthalene-D_8, acenaphthene-D_{10}, phenanthrene-D_{10}, pyrene-D_{10}, chrysene-D_{12}, perylene-D_{12} and benzo[g,h,i]perylene-D_{12}), two deuterated-OPAHs (benzophenone-D_5 and anthraquinone-D_8) and three deuterated-NPAHs (2-nitrofluorene-D_9, 3-nitrofluoranthene-D_9 and 6-nitrochrysene-D_{11}) as internal standards. Samples were extracted twice by pressurized liquid extraction (ASE 200, Dionex, Sunnyvale, CA, USA) using dichloromethane (DCM) as the extraction solvent. The ASE instrumental conditions, purification procedures and analysis by gas chromatography/mass spectrometry (GC/MS) followed the method used by Bandowe et al. (2014). A total of 29 PAHs, 15 OPAHs, 11 NPAHs and 4AZAs were measured and the monitored and qualifier ions used for detection and quantification are shown in Table S2.

2.3. Quality assurance/quality control

All glassware used during sample preparation and analysis were machine-washed and baked overnight at 250 °C in an oven. Solvents were pesticide residue grade (J.T. Baker, Center Valley, PA, USA).

For carbon analysis, the Carbon Analyzer was calibrated with known quantities of CH_4 every day. Every 10th sample in a measurement sequence which also included samples from other locations not included in this study was analyzed in duplicate to check for analytical precision. Precision, expressed as the relative standard deviation of the mean, was <5% for TC, <8% for OC and EC, and <10% for char and soot.

For the analysis of PACs, several laboratory and field blanks (QFFs and PUFs) were measured to verify potential contamination (Table S3). Average field values of the 59 target PACs were subtracted from samples. The average recoveries of the deuterated internal standards were 90% [range: 57% (benzo[g,h,i]perylene-D_{12}) to 140% (anthraquinone-D_8)] in filters and 100% [range: 55% (Naphthalene-D_8) to 135% (perylene-D_{12})] in PUFs. The limit of detection was calculated as a signal to noise ratio of 3:1 following Bandowe et al. (2014) (Table S3).

2.4. Calculations and properties of PACs

The characteristics of 59 PACs and the toxicity equivalency factors (TEFs) of selected PACs are summarized in Table S2. The sum of all 29 PAHs, 15 OPAHs, 11 NPAHs, 4 AZAs, low molecular weight parent PAHs (2–3 rings), high molecular weight parent PAHs (4–7 rings) and 16 U.S. EPA priority PAHs are referred to as $\sum 29$PAHs, $\sum 15$OPAHs, $\sum 11$NPAHs, $\sum 4$AZAs, LMW, HMW and $\sum 16$PAHs, respectively.

2.4.1. Calculation of gas-particle partitioning

The distribution of a PACs between the gaseous and particulate phases is described by the partitioning coefficient (K_p) (Pankow, 1987; Terzi and Samara, 2004):

$$K_p = \left(C_p/TSP\right)/C_g \tag{1}$$

where C_p and C_g are the concentrations of the target compound in the particulate and gas phases (ng m^{-3}), and TSP is the mass of total suspended particulate matter in the air (μg m^{-3}).

Adsorption and absorption are the two classical mechanisms that govern the association between PACs and atmospheric aerosols, and hence gas-particle partitioning (Goss and Schwarzenbach, 1998; Shen et al., 2011b). For both mechanisms there is a linear relationship

between log K_p and log P_L^0 (Pankow, 1987, 1994a,b; Pankow and Bidleman, 1991; Terzi and Samara, 2004):

$$log \ K_p = m_r log P_L^0 + b_r \tag{2}$$

where P_L^0 is the sub-cooled liquid vapor pressure of a particular compound. A linear regression of $logK_p$ on $logP_L^0$ was calculated for individual PAHs, OPAHs and NPAHs to determine their m_r and b_r values after normal distribution of the data sets was verified.

2.4.2. Carcinogenic risk assessment

Carcinogenic risk was estimated using the TEFs, and was calculated following the method of Albinet et al. (2008):

$$\text{Carcinogenic risk} = \sum_i (C_i \times TEF)_i \times UR_{BaP} \tag{3}$$

where C_i and TEF_i are the individual concentration and TEF value of the target PAC (Table S2), respectively. To the best of our knowledge, no better data were available for the risk assessment of OPAHs. UR_{BaP} (unit risk) is defined as the number of people at risk of contracting cancer from the inhalation of a BaP equivalent concentration of 1 ng m^{-3} within a lifetime of 70 years, and has a value of 1.1×10^{-6} (ng m^{-3})$^{-1}$ according to the California Environmental Protection Agency (OEHHA, 1994).

3. Results and discussion

3.1. Concentrations of TSP and carbon factions

The mass concentrations of TSP and the four carbon fractions in both March and September are summarized in Table 1 and Fig. 1. The average mass concentration of TSP in March was 416.5 ± 125.5 μg m^{-3} (average ± standard deviation), which was much higher than in September (151.7 ± 63.4 μg m^{-3}) ($p = 0.014$) (Table 1), indicating serious particulate pollution in March. These values were comparable with those reported in previous studies in Xi'an by Zhang et al. (2002) and Shen et al. (2009). The average OC and EC concentrations were 42.8 ± 14.5 and 12.1 ± 2.8 μg m^{-3} in March, contributing 10.3% and 2.9% of the mass of TSP, respectively. Although OC and EC concentrations in March were higher than in September (Table 1), their contribution to the TSP was reversed (17.5% for OC and 5.1% for EC in September). Average char and soot concentrations at Xi'an were 11.0 ± 2.6 and 1.2 ± 0.3 μg m^{-3} in March, respectively, which were also higher than those in September

Table 1
Summary of the concentrations of the mass and carbon fractions of total suspended particle (TSP) and meteorological conditions during sampling in Xi'an.

Compounds	March	September
Mass (μg m^{-3})	416.5 ± 125.5	151.7 ± 63.4
Carbon factions (μg m^{-3})		
TC[a]	54.9 ± 17.1	26.5 ± 17.3
OC[a]	42.8 ± 14.5	18.8 ± 12.6
EC[a]	12.1 ± 2.8	7.8 ± 4.9
Char	11.0 ± 2.6	7.2 ± 4.5
Soot	1.2 ± 0.3	0.6 ± 0.4
OC/EC	3.5 ± 0.5	2.3 ± 0.9
Char/soot	9.6 ± 2.3	12.7 ± 0.8
Meteorological conditions		
T[b] (°C)	13.9 ± 1.9	19.5 ± 1.6
RH[b] (%)	66.7 ± 17.5	70.6 ± 16.3
P[b] (hPa)	975.1 ± 2.9	971.2 ± 3.1
WS[b] (m/s)	1.3 ± 0.4	1.4 ± 0.2

[a] TC, OC and EC are total carbon, organic carbon, and elemental carbon, respectively.
[b] T, RH, P and WS here represent temperature, relative humidity, pressure and wind speed in the ambient environment during sampling, respectively.
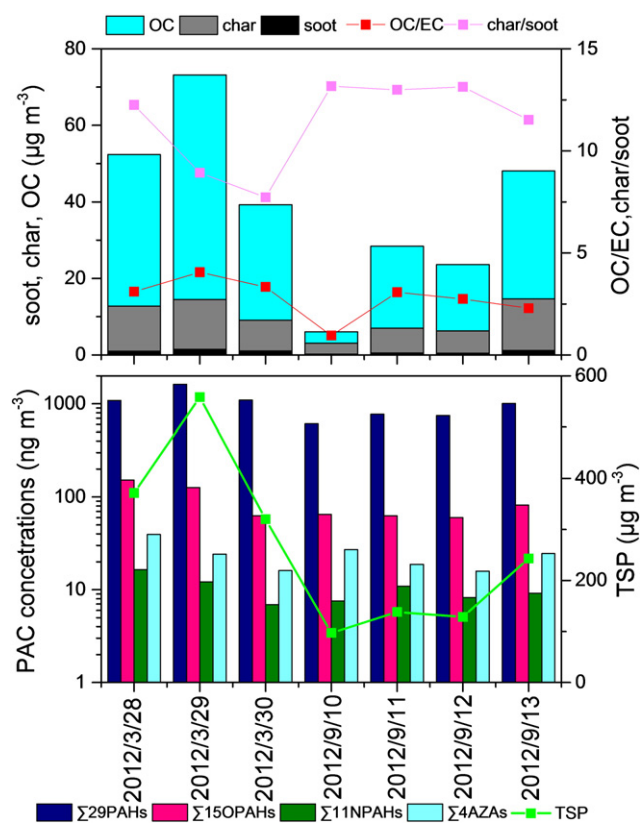
Fig. 1. Concentrations of PACs, TSP, carbon fractions and concentration ratios of OC/EC and char/soot at an urban sampling location in Xi'an. The sum of concentrations of char plus soot is EC concentration, while the sum of concentrations of OC, char and soot equals TC concentration.

(Table 1). Concentrations of OC, EC (char + soot), char and soot paralleled those of TSP (Fig. 1). The highest concentrations of TSP and the carbon fractions were recorded on 29 March, while the lowest loading was recorded on 10 September (Fig. 1) because of precipitation scavenging (18.8 mm rainfall, Table S1), which is an important factor that influences atmospheric aerosol concentrations (Armalis, 1999; Han et al., 2010). Wind is another factor that affects particle concentrations in ambient air (Cao et al., 2009; Ragosta et al., 2002). TSP and carbon fractions likely accumulated in ambient air at low wind speeds (<1.3 m s^{-1}) or when non-directional wind dominated and pollutants recycled in the Guanzhong Basin (Fig. S1) such as on 29 March 2012 (Fig. S2). At higher wind speeds or when the directional dominant wind (south-west and north-west in March and September, respectively (Wang et al., 2012)) controlled, TSP and carbon fractions were diluted (Table S1, Fig. S2). The influence of precipitation and wind explains the variation in the concentrations of TSP and its associated pollutants during several days (Fig. 1A). Other factors, e.g., emission differences and dust storms, also can affect the concentrations of TSP and the carbon fractions, leading to higher values in March (Shen et al., 2009). Although 15 November to 15 March is the period when central heating is used in buildings in Xi'an, there were some occasions in the sampling period during which particles were also emitted by domestic heating of rural families and coal or petroleum combustion in some public buildings (e.g., hospitals). The magnitude of such non-centralized heating is higher in the colder periods (March) than in the slightly hotter period (September, Tables 1 and S1).

The measured OC/EC and char/soot ratios are shown in Table 1 and Fig. S3. These ratios are usually used as markers to distinguish between sources of aerosol (Cao et al., 2005; Han et al., 2010; Shen et al., 2010). An OC/EC value of 2.7 indicates coal combustion, 1.1 indicates

combustion in motor vehicle engines (Watson et al., 2001) and 9.0 indicates biomass burning (Cachier et al., 1989). The OC/EC ratio is not only influenced by the fuel used (primary emissions), but also by the formation of secondary organic aerosols. The OC/EC ratio is not universally suitable for the identification of primary sources of carbonaceous aerosol (Han et al., 2010). Han et al. (2010) proposed the char/soot ratio to identify primary sources because both atmospheric char and soot concentrations are controlled by primary emission sources and have different removal rates by deposition. The char/soot ratio is less than 1 for combustion in a motor vehicle engine, 1.5 to 3.0 for residential coal combustion, 2.0 to 6.0 for domestic cooking, and much higher for biomass burning (Han et al., 2010). The OC/EC and char/soot ratios indicated that the atmospheric particles sampled in Xi'an during the study period mainly originated from a mixture of vehicle exhaust emissions, coal combustion and biomass burning (Fig. S3).

3.2. Occurrence and composition of PACs

3.2.1. PAHs

The average total concentrations (gaseous + particulate) of $\sum 29$PAHs and $\sum 16$PAHs were 1267.0 ± 307.5 and 728.6 ± 131.9 ng m^{-3} in March, which were higher than the levels recorded in September (Table 2, Fig. 1). The average concentrations of $\sum 16$PAHs (gaseous + particulate) in both months were higher than those reported from other cities, such as Chicago, USA (428 ± 240 ng m^{-3} in June to October, 1995) (Odabasi et al., 1999), Kocaeli, Turkey (108 ng m^{-3} in summer 2006) (Gaga et al., 2012) and Guangzhou, China (337 ± 137 ng m^{-3}) (Lee et al., 2001). The average concentration of $\sum 16$PAHs (gaseous + particulate) accounted for 58% and 70% of the $\sum 29$PAHs concentration in March and September, respectively. This implies that the measurement of just the 16 U.S. EPA priority PAHs may miss a large fraction of the total PAHs, such as methyl-PAHs in both months, and especially the cooler time (Table S4). Gaseous $\sum 29$PAHs, $\sum 16$PAHs, LMW, and HMW accounted for 88%, 85%, 99% and 30% of the total gaseous plus particulate phases in March, and 91%, 89%, 99% and 46% in September, which suggests that most of the measured PAHs (especially LMW) were present in the gaseous phase and the proportion of the total compound concentration in the gaseous phase increased with increasing temperature because of enhanced volatilization. Phenanthrene (22%), 1,3-dimethylnaphthalene (14%) and naphthalene (10%) were the dominant PAHs in March, which were similar to September, while dibenzo[a,h]anthracene, perylene and 1,2,3,4-tetrahydronaphthalene were the least abundant in both months (Fig. 2). The pattern of PAH concentrations in the two months was similar to each other ($r^2 = 0.73$, $p < 0.001$, linear regression) suggesting similar sources of the PAHs in the two sampling periods.

3.2.2. OPAHs

The average concentration of $\sum 15$OPAHs (gaseous + particulate) was 113.8 ± 46.1 ng m^{-3} in March, which was higher than in September (67.4 ± 9.8 ng m^{-3}) (Table 2, Fig. 1). This was almost one order of magnitude lower than the average concentration of $\sum 29$PAHs, but was higher than that reported in Birmingham, UK (29.1 ng m^{-3} in January, 2010) (Delgado-Saborit et al., 2013), Texas, USA (0.56 ng m^{-3} in March, 1991) (Wilson et al., 1995) and Singapore (4.14 ± 1.42 ng m^{-3} in November, 2006) (He et al., 2010). Gaseous $\sum 15$OPAHs accounted for 78% and 76% of the total $\sum 15$OPAHs concentrations in gaseous + particulate phases in March and September, respectively. These values were lower than the percentages of $\sum 29$PAHs and $\sum 16$PAHs in the gaseous phase, because the measured OPAHs had a high molecular weight and therefore preferably occurred in the particulate phase (Albinet et al., 2008). 9-Fluorenone (42%), 1-indanone (17%), 1,4-naphthoquinone (10%) and 9,10-anthraquinone (7.3%) were the most abundant OPAHs, while 5,12-naphthacenequinone (1.2%), 1,8-naphthalic anhydride (0.5%) and 2-
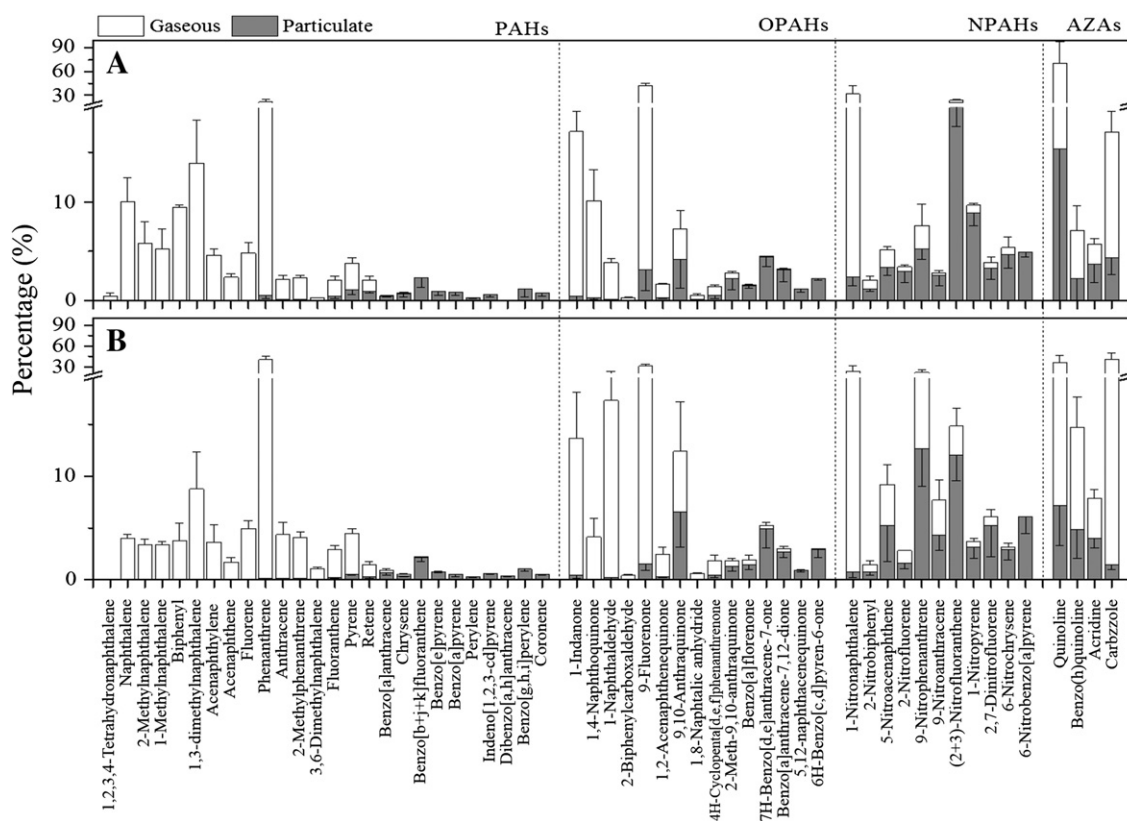
Fig. 2. Composition of the mixtures of 29 PAHs, 15 OPAHs, 11 NPAHs and 4 AZAs in ambient gaseous and particulate phases in March (A) and September (B) at an urban sampling location in Xi'an.

biphenylcarboxaldehyde (0.5%) were the least abundant in March (Fig. 2). The pattern of OPAH concentrations in March was similar to that in September (Fig. 2) ($r^2 = 0.77$, $p < 0.0001$, linear regression), as was also found for PAHs.

3.2.3. NPAHs

The average concentration of $\sum 11$NPAHs (gaseous ± particulate) was 11.8 ± 4.8 ng m^{-3} in March, which was slightly higher than in September (9.0 ± 1.5 ng m^{-3}) (Table 2, Fig. 1). These values were nearly two orders of magnitude lower than the average concentration of $\sum 29$PAHs, and were higher than those reported from Texas, USA (0.28 ng m^{-3}) (Wilson et al., 1995) and Toronto, Canada (0.1 ng m^{-3}) (Klein et al., 2006). Gaseous $\sum 11$NPAH concentrations were similar to particulate concentrations in both periods (Table 2),

which was not true for gaseous $\sum 29$PAHs and $\sum 15$OPAHs. 1-Nitronaphthalene (32%), (2 + 3)-nitrofluoranthene (23%) and 1-nitropyrene (10%) were the most abundant compounds among the NPAHs, while 2,7-dinitrofluorene (3.9%), 9-nitroanthracene (2.8%), and 2-nitrobiphenyl (2.1%) were the least abundant in March (Fig. 2). The concentration pattern in March was similar to that in September ($r^2 = 0.53$, $p = 0.011$, linear regression).

3.2.4. AZAs

The average concentration of $\sum 4$AZAs was 26.5 ± 11.8 ng m^{-3} in March, which was slightly higher than in September (21.6 ± 5.1 ng m^{-3}) (Table 2, Fig. 1) and the concentration of gaseous $\sum 4$AZAs was almost four times higher than the particulate $\sum 4$AZAs concentration in both months. Quinoline, benzo[h]quinoline, acridine

Table 2
Concentration of polycyclic aromatic hydrocarbons (PAHs) and their derivatives (OPAHs, NPAHs, AZAS) in the gaseous (G), particulate (P) and gaseous plus particulate (G + P) phases at an urban sampling location in Xi'an.

	March				September			
	G	P	G/P[a]	G + P	G	P	G/P[a]	G + P
LMW[b]	687.4 ± 149.4	9.0 ± 3.5	76.25	696.4 ± 148.0	485.5 ± 84.7	2.8 ± 2.8	171.18	488.3 ± 86.3
HMW[b]	54.4 ± 9.5	124.6 ± 40.5	0.44	178.9 ± 49.3	55.2 ± 6.9	64.5 ± 22.9	0.86	119.7 ± 27.3
$\sum$ 16PAHs[b]	621.6 ± 123.5	107.0 ± 34.5	5.81	728.6 ± 131.9	492.3 ± 68.1	59.0 ± 20.5	8.34	551.3 ± 84.9
$\sum$ 29PAHs[b]	1117.8 ± 307.6	149.2 ± 42.9	7.49	1267.0 ± 307.5	713.0 ± 138.2	71.7 ± 27.2	9.95	784.7 ± 165.1
$\sum$ 15OPAHs[b]	89.2 ± 43.0	24.6 ± 3.9	3.62	113.8 ± 46.1	51.0 ± 8.0	16.2 ± 6.0	3.14	67.4 ± 9.8
$\sum$ 11NPAHs[b]	4.9 ± 2.5	6.9 ± 2.3	0.70	11.8 ± 4.8	4.0 ± 0.8	5.0 ± 1.4	0.80	9.0 ± 1.5
$\sum$ 4AZAs[b]	21.5 ± 14.8	5.0 ± 4.0	4.31	26.5 ± 11.8	18.0 ± 5.8	3.6 ± 1.6	5.07	21.6 ± 5.1

[a] G/P means the ratio of the average concentration in the gaseous to that in the particulate phase.
[b] LMW is the sum of the naphthalene, acenaphthylene, acenaphthene, fluorene, phenanthrene and anthracene concentrations; HMW is the sum of fluoranthene, pyrene, benzo[a]anthracene, chrysene, benzo[bjk]fluoranthene, benzo[e]pyrene, benzo[a]pyrene, perylene, indeno[1,2,3-cd]pyrene, dibenzo[a,h]anthracene, benzo[g,h,i]perylene and coronene concentrations. $\sum$16PAHs is the sum of the naphthalene, acenaphthylene, acenaphthene, fluorene, phenanthrene, anthracene, fluoranthene, pyrene, benzo[a]anthracene, chrysene, benzo[bjk]fluoranthene, benzo[a]pyrene, indeno[1,2,3-cd]pyrene, dibenzo[a,h]anthracene and benzo[g,h,i]perylene concentrations; $\sum$29PAHs, $\sum$15OPAHs, $\sum$11NPAHs, $\sum$4AZAs are the sums of 29 parent- and alkyl-PAHs, 15 oxygenated PAHs, 11 nitrated PAHs and 4 azaarenes concentrations, respectively.

Table 3
Selected mean concentration ratios (± standard deviations) of PAHs, OPAHs, NPAHs and of PAHs to the carbon fractions in the atmosphere of Xi'an.

Ratio[a]	March	September
LMW/HMW[b]	3.806 ± 0.953	4.247 ± 0.428
$\sum$ 15OPAHs/$\sum$ 29PAHs[b]	0.079 ± 0.025	0.087 ± 0.013
$\sum$ 11NPAHs/$\sum$ 29PAHs[b]	0.010 ± 0.005	0.012 ± 0.002
$\sum$ 11NPAHs/$\sum$ 15OPAHs[b]	0.105 ± 0.008	0.135 ± 0.028
Benzo[e]pyrene/benzo[a]pyrene	1.087 ± 0.133	1.732 ± 0.405
Benzo[ghi]perylene/benzo[a]pyrene	1.346 ± 0.502	2.324 ± 0.720
9-Fluorenone/fluorene	0.770 ± 0.177	0.543 ± 0.062
9,10-Anthraquinone/anthracene	0.287 ± 0.073	0.037 ± 0.008
Benzo[a]anthracene-7,12-dione/benzo[a]anthracene	0.531 ± 0.196	0.286 ± 0.077
1,2-Acenaphthenequinone/acenaphthene	0.067 ± 0.037	0.140 ± 0.072
1-Nitronapthalene/napthalene	0.037 ± 0.032	0.067 ± 0.023
5-Nitroacenaphethene/acenaphthene	0.022 ± 0.013	0.062 ± 0.032
2-Nitrobiphenyl/biphenyl	0.003 ± 0.001	0.006 ± 0.004
2-Nitrofluoranthene/fluoranthene	0.007 ± 0.003	0.007 ± 0.002
9-Nitrophenanthrene/nitrophenanthrene	0.003 ± 0.001	0.006 ± 0.002
9-Nitroanthracene/anthracene	0.011 ± 0.004	0.021 ± 0.007
6-Nitrochrysene/chrysene	0.064 ± 0.026	0.070 ± 0.012
6-Nitrobenzo[a]pyrene/benzo[a]pyrene	0.052 ± 0.004	0.157 ± 0.052
2-Nitrofluorene/1-nitropyrene	2.423 ± 0.224	4.076 ± 0.578
$\sum$ 29PAHs/TC[b]	0.024 ± 0.004	0.045 ± 0.037
$\sum$ 29PAHs/OC[b]	0.030 ± 0.005	0.079 ± 0.086
$\sum$ 29PAHs/EC[b]	0.106 ± 0.019	0.124 ± 0.053
$\sum$ 29PAHs/char	0.118 ± 0.023	0.133 ± 0.057
$\sum$ 29PAHs/soot	1.096 ± 0.038	1.716 ± 0.793

[a] Individual values and the sum of PAHs, OPAHs, NPAHs and AZAs concentrations refer to the gaseous plus particulate phase.

[b] LMW is the sum of the naphthalene, acenaphthylene, acenaphthene, fluorene, phenanthrene and anthracene concentrations; HMW is the sum of the fluoranthene, pyrene, benzo[a]anthracene, chrysene, benzo[b + j + k]fluoranthene, benzo[e]pyrene, benzo[a]pyrene, perylene, indeno[1,2,3-cd]pyrene, dibenzo[a,h]anthracene, benzo[g,h,i]perylene and coronene concentrations. $\sum$ 15OPAHs, $\sum$ 29PAHs and $\sum$ 11NPAHs are the sum of 15 oxygenated-PAHs, 29 parent- and alkyl-PAHs and 11 nitrated-PAHs concentrations, respectively. TC, OC, EC are acronyms for total carbon, organic carbon and elemental carbon, respectively.

and carbazole, the four AZA compounds investigated in this study, accounted for 70%, 7%, 6% and 17% in March and 36%, 15%, 8% and 41% of the $\sum$ 4AZAs concentrations in September, respectively (Fig. 2).

Both gaseous and particulate $\sum$ 29PAHs displayed a similar daily variation to TSP and their carbon fractions (Table S5, Fig. 1), which is probably because PAHs (both gaseous and particulate) were mainly emitted from primary sources associated with particles and their carbon contents (e.g., OC, char and soot). The concentrations of particulate $\sum$ 15OPAHs and $\sum$ 11NPAHs were significantly correlated with those of the carbon fractions, but the gaseous $\sum$ 15OPAHs and $\sum$ 11NPAHs were not (Table S5) suggesting that particulate polar PACs (OPAHs and NPAHs) were co-emitted with carbon fractions and co-sorbed to carbon fractions and therefore PACs and carbon fractions showed a similar fate. PACs in the gaseous phase in contrast are susceptible to other process such as photochemical transformation and deposition by gas–solid phase partitioning to terrestrial surfaces that are markedly different from the fate of carbon fractions in the particulate phase.

PAC concentration ratios have been used to distinguish their sources in air (Albinet et al., 2008; Kim et al., 2012). A higher BeP/BaP ratio in September (Table 3) suggests photochemical aging of PACs in ambient air, because this ratio is ~1 close to sources, and increases during "aging" because BaP is degraded faster than BeP in the environment (Kamens et al., 1988; Lammel et al., 2010). The concentration ratios of $\sum$ 11NPAHs/$\sum$ 29PAHs and individual NPAH to parent-PAHs were higher in September than in March (Tables 3 & S6), which also indicates a large contribution from NPAHs formed from photochemical reactions of their parent-PAHs (Huang et al., 2014). The concentration ratios of $\sum$ 15OPAHs/$\sum$ 29PAHs and most individual OPAHs to their parent-PAHs were lower in September than in March, whereas the $\sum$ 11NPAHs/$\sum$ 15OPAHs concentration ratio displayed an opposite pattern (Tables 3 & S6). This suggests that OPAHs mainly originated

from primary emission sources and the more intense photochemical activity in September therefore did not lead to significant formation of OPAHs from their parent-PAHs. Alternatively, it is possible that both the OPAHs and their parent-PAHs are equally susceptible to photochemical degradation, which would prevent any excess accumulation of OPAHs. Furthermore, relatively high OPAH emissions from residential cooking and heating due to differences in the amount of oxygen supplied, result in lower combustion efficiencies and relatively high temperatures in enclosed residential stoves (Shen et al., 2011a). Other concentration ratios, such as those of $\sum$ 29PAHs, $\sum$ 15OPAHs, $\sum$ 11NPAHs and $\sum$ 4AZAs in relation to TC, OC, EC, char and soot were higher in September indicating that these carbon fractions contain more PACs (Table S6). This can be explained by: 1) more PACs being evaporated from storage pools (e.g., soil) in September because of the higher ambient temperature (Wang et al., 2011b), and 2) the TSP could contain more carbon in March because dust storms, which occasionally occur in the Xi'an region in March, could introduce carbonaceous materials from the surrounding areas (Shen et al., 2009).

3.3. Gas/particle partitioning of PACs

The fractions of individual PAHs, OPAHs and NPAHs of the total atmospheric concentrations in the particulate phase depended strongly on the molecular weight (MW), and the relationships between gaseous and particulate phases displayed variations among the two sampling periods (Fig. 3). All PAHs, OPAHs and NPAHs were shifted to the particulate phase to some extent in March (Fig. 3) because of the lower temperature (Table S1), which was also observed in French alpine valleys (Albinet et al., 2008) and Birmingham, UK (Delgado-Saborit et al., 2013). Normally, low molecular weight compounds (i.e. MW <200 g mol^{-1}) mainly occurred in the gaseous phase, whereas high molecular weight compounds (MW >240 g mol^{-1}) were detected in the particulate phase during the two studied months. The fractions of particulate PACs were also plotted and a sigmoidal logistic function with other physicochemical properties, such as log P_L^0, K_{OW} and Henry's Law constant (H) was fitted (Fig. S4). They all displayed similar trends to that shown in Fig. 3 except for the relationship between the fraction of total atmospheric concentrations in particulates and H for OPAHs, which suggested that MW, log P_L^0 and K_{OW} might all be suitable predictors of gas/particle partitioning (Delgado-Saborit et al., 2013).

The slopes (m_r) and intercepts (b_r) of the regression lines of log K_p on log P_L^0 for PAHs, OPAHs, NPAHs and PACs were calculated for the two study months (Fig. 4) and for individual days (Table S7). Absorption into the organic matter in particles and adsorption onto the surface of particles occurred simultaneously for PAHs and OPAHs, and absorption occurred more frequently in September as indicated by the slope values (Fig. 4). In contrast, absorption was the main mechanism for the association of NPAHs with particles in both periods (Fig. 4). More PACs are expected to partition to the gaseous phase in September because of the higher ambient temperature (Table S1), which could introduce a lower K_p and therefore a less negative m_r in September (Fig. 4). m_r was also significantly correlated with b_r for both OPAHs ($r = 0.84$, $p = 0.018$) and NPAHs ($r = 0.90$, $p = 0.006$), but not PAHs ($r = 0.74$, $p = 0.057$), suggesting a relationship between m_r and b_r for OPAHs and NPAHs. The slope and intercept of the linear regression of b_r on m_r for PAHs were 3.69 and -1.37, respectively, which were consistent with published data (Pankow and Bidleman, 1992; Terzi and Samara, 2004), but higher than the values for OPAHs (slope = 3.12 and intercept = -1.53) and NPAHs (slope = 2.37 and intercept = -2.09).

3.4. Carcinogenic risk of PACs

Because there are no TEF values for OPAHs and AZAs available, the published TEF values of selected PAHs and NPAHs (Table S2) were used to evaluate the carcinogenic risk in this study. The total risk of
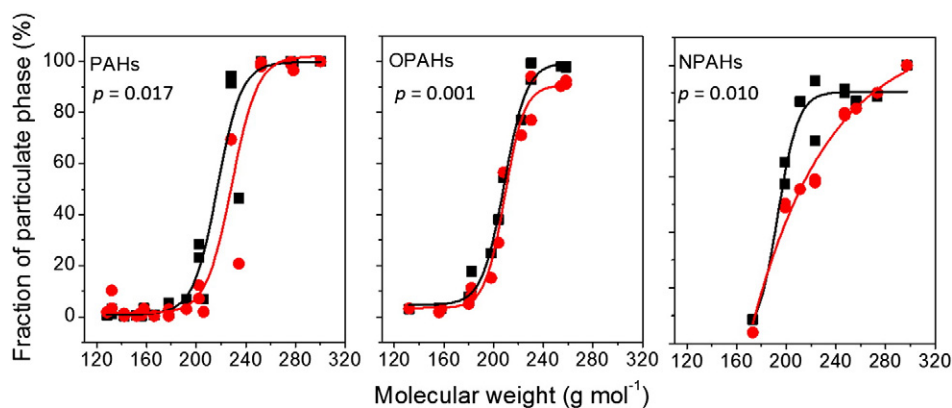
Fig. 3. Fraction of PAHs, OPAHs and NPAHs concentrations in the particulate fraction of their total atmospheric concentrations (gaseous + particulate) according to their molecular weight in March (black square) and September (red dot) 2012 at an urban sampling location in Xi'an. *p* values refer to t-tests of paired samples in March and September.

the sum of PAHs and NPAHs was 4.4×10^{-5} in March, which was higher than in September (2.8×10^{-5}) (Fig. 5, A). There was also a higher carcinogenic risk posed by the atmospheric concentrations of both PAHs and NPAHs in March than in September. Although the concentrations of NPAHs (gaseous + particulate) were two orders of magnitude lower than those of PAHs, the carcinogenic risk of NPAHs (gaseous + particulate) contributed a large amount of the total carcinogenic risk of PACs. For example, NPAHs accounted for 17% and 11% of the total carcinogenic risk (NPAHs + PAHs) in March and September, respectively. The carcinogenic risk of gaseous PACs accounted for 29% and 44% of the total risk in March and September, respectively, indicating that gaseous PACs contributed a large proportion of the total carcinogenic risk, which increased further at higher ambient temperatures. In the

future, any risk assessment of PACs should consider the impact of gaseous compounds as well as particulates.

4. Conclusions

The concentrations of $\sum 29$PAHs were one to two orders of magnitude higher than those of $\sum 15$OPAHs, $\sum 11$NPAHs and $\sum 4$AZAs in both March and September at the selected urban location in Xi'an. Higher $\sum 29$PAHs, $\sum 15$OPAHs, $\sum 11$NPAHs and $\sum 4$AZAs concentrations were recorded in March, as well as of TSP and carbon fractions (OC, EC and soot). All of the pollutants mainly originated from a mixture of vehicle exhausts, coal combustion and biomass burning in both sampling periods. Secondary formation (e.g., by photochemical reactions)
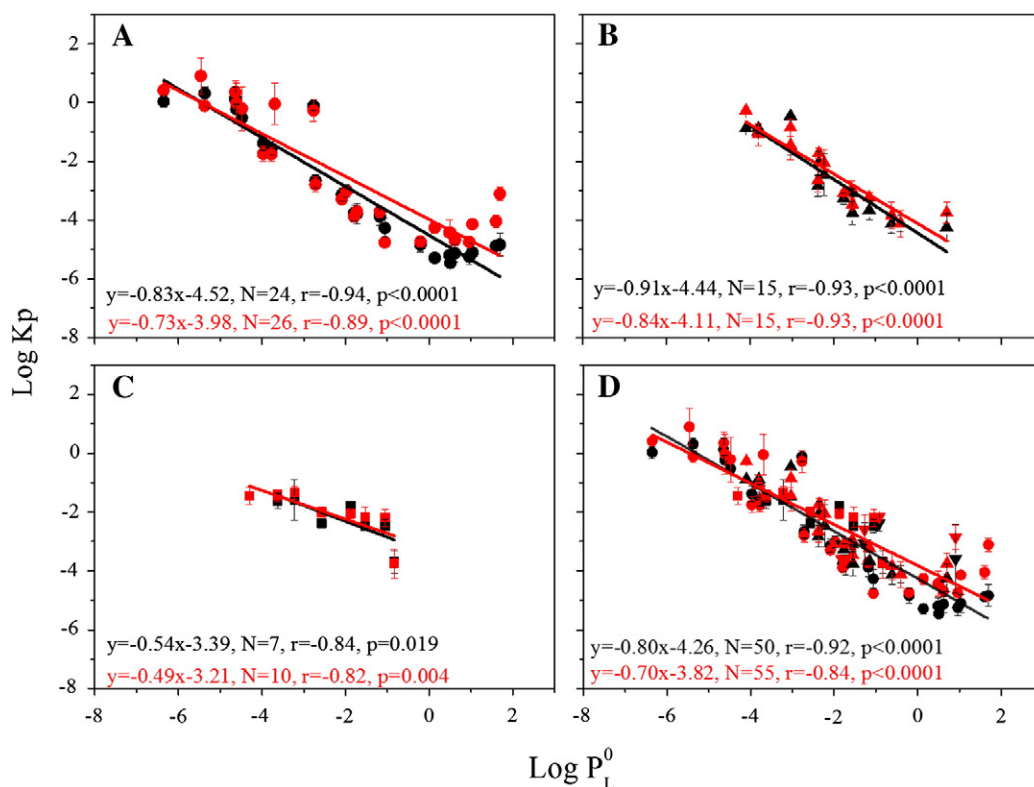
Fig. 4. Linear regression of log K_p on log P_L^0 for PAHs (A, circle), OPAHs (B, up-triangle), NPAHs (C, square) and all PACs (D, down-triangle represents AZAs) in March (black) and September (red).
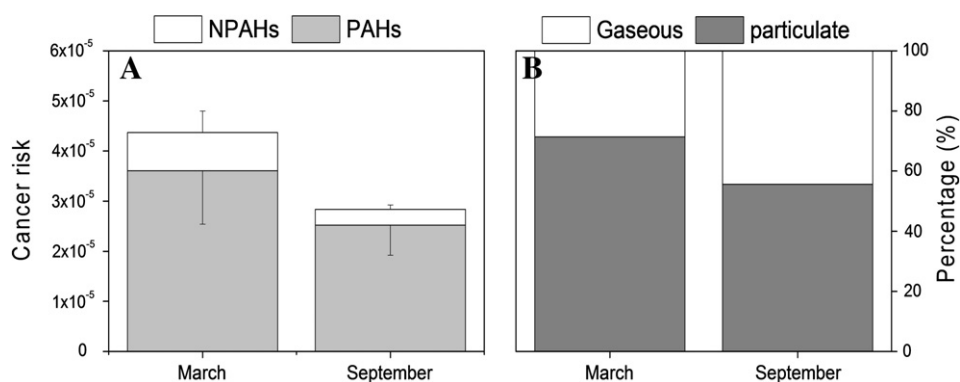
Fig. 5. Total cancer risk calculated from the ambient concentration of 20 PAHs and 6 NPAHs (left) and the contribution of gaseous and particulate-bound compounds (right).

also contributed to the atmospheric concentrations of polar compounds (i.e. OPAHs and NPAHs) in September. Molecular weight was a suitable predictor of phase partitioning and more absorption occurred in September for all PACs, although both absorption into particulate organic matter and adsorption onto the surface of particles occurred in both periods. The total carcinogenic risk of PAHs and NPAHs was higher in March. Gaseous compounds contributed a large fraction of the total risk and their contribution increased as the ambient temperature increased. Future carcinogenic risk assessment in air should include the impact of gaseous compounds as well as particulates.

Acknowledgments

Appendix A. Supplementary data

The Supplementary information describes the detailed protocol of the PACs analysis method, provides a map of the sampling site in Fig. S1 and summarizes atmospheric properties during sampling periods in Table S1. Tables S2–S4 summarize the names, abbreviations, properties, blanks and concentrations of 59 PACs. Correlation coefficients between atmospheric concentrations of PACs and the carbon fractions, meteorological factors and gaseous components are given in Table S5, while selected concentration ratios of individual compounds or sum of compounds are summarized in Table S6. A wind rose showing the wind directions and wind speeds during sampling is plotted for individual days in Fig. S2. A plot of the char/soot concentration ratio against OC/EC is presented in Fig. S3. The particulate fractions of the total atmospheric concentrations of PAHs, OPAHs and NPAHs are plotted against their sub-cooled vapor pressure (P_L^0), and K_{OW} values and Henry's Law Constant (H) are presented in Fig. S4. The coefficients of the regression lines of $logK_p$ on $logP_L^0$ for PACs are shown in Table S7, and the correlation coefficients of PACs concentrations with other factors are presented in Table S8. Supplementary data associated with this article can be found in the online version. Supplementary data associated with this article can be found in the online version, at http://dx.doi.org/10.1016/j.scitotenv.2014.10.054. These data include Google maps of the most important areas described in this article.

References

Albinet A, Leoz-Garziandia E, Budzinski H, Villenave E. Polycyclic aromatic hydrocarbons (PAHs), nitrated PAHs and oxygenated PAHs in ambient air of the Marseilles area (South of France): concentrations and sources. Sci Total Environ 2007;384: 280–92.

Albinet A, Leoz-Garziandia E, Budzinski H, Villenave E, Jaffrezo JL. Nitrated and oxygenated derivatives of polycyclic aromatic hydrocarbons in the ambient air of two French alpine valleys: part 1: concentrations, sources and gas/particle partitioning. Atmos Environ 2008;42:43–54.

Armalis S. Wet deposition of elemental carbon in Lithuania. Sci Total Environ 1999;239: 89–93.

Atkinson R, Arey J. Atmospheric chemistry of gas-phase polycyclic aromatic hydrocarbons: formation of atmospheric mutagens. Environ Health Perspect 1994;102: 117–26.

Bandowe BAM, Rückamp D, Bragança MAL, Laabs V, Amelung W, Martius C, et al. Naphthalene production by microorganisms associated with termites: evidence from a microcosm experiment. Soil Biol Biochem 2009;41:630–9.

Bandowe BAM, Meusel H, Huang R-j, Ho K, Cao J, Hoffmann T, et al. PM$_{2.5}$-bound oxygenated PAHs, nitro-PAHs and parent-PAHs from the atmosphere of a Chinese megacity: seasonal variation, sources and cancer risk assessment. Sci Total Environ 2014; 473–474:77–87.

Bleeker EAJ, Van Der Geest HG, Klamer HJC, De Voogt P, Wind E, Kraak MHS. Toxic and genotoxic effects of azaarenes: isomers and metabolites. Polycycl Aromat Compd 1999;13:191–203.

Cachier H, Brémond M-P, Buat-Ménard P. Carbonaceous aerosols from different tropical biomass burning sources. Nature 1989;340:371–3.

Cao JJ, Lee SC, Ho KF, Zou SC, Fung K, Li Y, et al. Spatial and seasonal variations of atmospheric organic carbon and elemental carbon in Pearl River Delta Region, China. Atmos Environ 2004;38:4447–56.

Cao J, Wu F, Chow JC, Lee SC, Li Y, Chen SW, et al. Characterization and source apportionment of atmospheric organic and elemental carbon during fall and winter of 2003 in Xi'an, China. Atmos Chem Phys 2005;5:3127–37.

Cao J-J, Zhu C-S, Chow JC, Watson JG, Han Y-M, Wang G-H, et al. Black carbon relationships with emissions and meteorology in Xi'an, China. Atmos Res 2009;94: 194–202.

Chow JC, Watson JG, Pritchett LC, Pierson WR, Frazier CA, Purcell RG. The DRI thermal/optical reflectance carbon analysis system: description, evaluation and applications in U.S. air quality studies. Atmos Environ A Gen Top 1993; 27:1185–201.

Delgado-Saborit JM, Alam MS, Godri Pollitt KJ, Stark C, Harrison RM. Analysis of atmospheric concentrations of quinones and polycyclic aromatic hydrocarbons in vapour and particulate phases. Atmos Environ 2013;77: 974–82.

Eisler R. Polycyclic aromatic hydrocarbon hazards to fish, wildlife, and invertebrates. A synoptic review. Biological Report 85(1.11). Laurel Maryland, USA: US Fish and Wildlife Service, Patuxent wildlife Research Center; 1987.

Gaga EO, Ari A, Dogeroglu T, Emel Cakrca E, Machin NE. Atmospheric polycyclic aromatic hydrocarbons in an industrialized city, Kocaeli, Turkey: study of seasonal variations, influence of meteorological parameters and health risk estimation. J Environ Monit 2012;14:2219–29.

Goldberg E. Black carbon in the environment: properties and distribution. New York: John Wiley & Sons; 1985.

Goss K-U, Schwarzenbach RP. Gas/solid and gas/liquid partitioning of organic compounds: critical evaluation of the interpretation of equilibrium constants. Environ Sci Technol 1998;32:2025–32.

Han Y, Cao J, Chow J, Watson J, An Z, Jin Z, et al. Evaluation of the thermal/optical reflectance method for discrimination between char-and soot-EC. Chemosphere 2007;69: 569–74.

Han YM, Cao JJ, Lee S, Ho K, An Z. Different characteristics of char and soot in the atmosphere and their ratio as an indicator for source identification in Xi'an, China. Atmos Chem Phys 2010;10:595–607.

Harner T, Bidleman TF. Octanol–air partition coefficient for describing particle/gas partitioning of aromatic compounds in urban air. Environ Sci Technol 1998;32: 1494–502.

He J, Zielinska B, Balasubramanian R. Composition of semi-volatile organic compounds in the urban atmosphere of Singapore: influence of biomass burning. Atmos Chem Phys 2010;10:11401–13.

Huang RJ, Zhang Y, Bozzetti C, Ho KF, Cao JJ, Han Y, et al. High secondary aerosol contribution to particulate pollution during haze events in China. Nature 2014;514:218–22.

Kamens RM, Guo Z, Fulcher JN, Bell DA. The influence of humidity, sunlight, and temperature on the daytime decay of polyaromatic hydrocarbons on atmospheric soot particles. Environ Sci Technol 1988;22:103–8.

Kim JY, Lee JY, Choi SD, Kim YP, Ghim YS. Gaseous and particulate polycyclic aromatic hydrocarbons at the Gosan background site in East Asia. Atmos Environ 2012;49:311–9.

Klein GP, Hodge EM, Diamond ML, Yip A, Dann T, Stern G, et al. Gas-phase ambient air contaminants exhibit significant dioxin-like and estrogen-like activity in vitro. Environ Health Perspect 2006;114:697–703.

Lammel G, Klánová J, Ilić P, Kohoutek J, Gasić B, Kovacić I, et al. Polycyclic aromatic hydrocarbons in air on small spatial and temporal scales — I. Levels and variabilities. Atmos Environ 2010;44:5015–21.

Lee SC, Ho KF, Chan LY, Zielinska B, Chow JC. Polycyclic aromatic hydrocarbons (PAHs) and carbonyl compounds in urban atmosphere of Hong Kong. Atmos Environ 2001; 35:5949–60.

Lima ALC, Farrington JW, Reddy CM. Combustion-derived polycyclic aromatic hydrocarbons in the environment—a review. Environ Forensic 2005;6:109–31.

Lundstedt S, White PA, Lemieux CL, Lynes KD, Lambert IB, Öberg L, et al. Sources, fate, and toxic hazards of oxygenated polycyclic aromatic hydrocarbons (PAHs) at PAH-contaminated sites. Ambio 2007;36:475–85.

Mastral AM, Callén MS. A review on polycyclic aromatic hydrocarbon (PAH) emissions from energy generation. Environ Sci Technol 2000;34:3051–7.

Nisbet ICT, LaGoy PK. Toxic equivalency factors (TEFs) for polycyclic aromatic hydrocarbons (PAHs). Regul Toxicol Pharmacol 1992;16:290–300.

Odabasi M, Vardar N, Sofuoglu A, Tasdemir Y, Holsen TM. Polycyclic aromatic hydrocarbons (PAHs) in Chicago air. Sci Total Environ 1999;227:57–67.

OEHHA. Health assessment part B. Benzo[a]pyrene as a toxic air contaminant. http://www.arb.ca.gov/toxics/id/summary/bap.pdf, 1994.

Pankow JF. Review and comparative analysis of the theories on partitioning between the gas and aerosol particulate phases in the atmosphere. Atmos Environ (1967) 1987; 21:2275–83.

Pankow JF. An absorption model of gas/particle partitioning of organic compounds in the atmosphere. Atmos Environ 1994a;28:185–8.

Pankow JF. An absorption model of the gas/aerosol partitioning involved in the formation of secondary organic aerosol. Atmos Environ 1994b;28:189–93.

Pankow JF, Bidleman TF. Effects of temperature, TSP and per cent non-exchangeable material in determining the gas-particle partitioning of organic compounds. Atmos Environ A Gen Top 1991;25:2241–9.

Pankow JF, Bidleman TF. Interdependence of the slopes and intercepts from log-log correlations of measured gas-particle partitioning and vapor pressure—I. Theory and analysis of available data. Atmos Environ A Gen Top 1992;26:1071–80.

Ragosta M, Caggiano R, D'Emilio M, Macchiato M. Source origin and parameters influencing levels of heavy metals in TSP, in an industrial background area of Southern Italy. Atmos Environ 2002;36:3071–87.

Ramírez N, Cuadras A, Rovira E, Marcé RM, Borrull F. Risk assessment related to atmospheric polycyclic aromatic hydrocarbons in gas and particle phases near industrial sites. Environ Health Perspect 2011;119:1110–6.

Ringuet J, Albinet A, Leoz-Garziandia E, Budzinski H, Villenave E. Reactivity of polycyclic aromatic compounds (PAHs, NPAHs and OPAHs) adsorbed on natural aerosol particles exposed to atmospheric oxidants. Atmos Environ 2012;61:15–22.

Rosenkranz H, Mermelstein R. The mutagenic and carcinogenic properties of nitrated polycyclic aromatic hydrocarbons. In: White CM, editor. Nitrated polycyclic aromatic hydrocarbons. Heidelberg: Huethig; 1985. p. 267–97.

Schnelle-Kreis J, Sklorz M, Orasche J, Stölzel M, Peters A, Zimmermann R. Semi volatile organic compounds in ambient $PM_{2.5}$. Seasonal trends and daily resolved source contributions. Environ Sci Technol 2007;41:3821–8.

Shen Z, Cao J, Arimoto R, Han Z, Zhang R, Han Y, et al. Ionic composition of TSP and $PM_{2.5}$ during dust storms and air pollution episodes at Xi'an, China. Atmos Environ 2009; 43:2911–8.

Shen Z, Cao J, Arimoto R, Han Y, Zhu C, Tian J, et al. Chemical characteristics of fine particles (PM_1) from Xi'an, China. Aerosol Sci Technol 2010;44:461–72.

Shen G, Tao S, Wang W, Yang Y, Ding J, Xue M, et al. Emission of oxygenated polycyclic aromatic hydrocarbons from indoor solid fuel combustion. Environ Sci Technol 2011a;45:3459–65.

Shen G, Wang W, Yang Y, Ding J, Xue M, Min Y, et al. Emissions of PAHs from indoor crop residue burning in a typical rural stove: emission factors, size distributions, and gas-particle partitioning. Environ Sci Technol 2011b;45:1206–12.

Terzi E, Samara C. Gas–particle partitioning of polycyclic aromatic hydrocarbons in urban, adjacent coastal, and continental background sites of Western Greece. Environ Sci Technol 2004;38:4973–8.

Wang W, Simonich S, Giri B, Chang Y, Zhang Y, Jia Y, et al. Atmospheric concentrations and air–soil gas exchange of polycyclic aromatic hydrocarbons (PAHs) in remote, rural village and urban areas of Beijing–Tianjin region, North China. Sci Total Environ 2011a;409:2942–50.

Wang W, Jariyasopit N, Schrlau J, Jia Y, Tao S, Yu T-W, et al. Concentration and photochemistry of PAHs, NPAHs, and OPAHs and toxicity of $PM_{2.5}$ during the Beijing Olympic Games. Environ Sci Technol 2011b;45:6887–95.

Wang X, Shen Z, Cao J, Zhang L, Liu L, Li J, et al. Characteristics of surface ozone at an urban site of Xi'an in Northwest China. J Environ Monit 2012;14:116–26.

Watson JG, Chow JC, Houck JE. $PM_{2.5}$ chemical source profiles for vehicle exhaust, vegetative burning, geological material, and coal burning in Northwestern Colorado during 1995. Chemosphere 2001;43:1141–51.

Wilcke W. Global patterns of polycyclic aromatic hydrocarbons (PAHs) in soil. Geoderma 2007;141:157–66.

Wilcke W, Müller S, Kanchanakool N, Niamskul C, Zech W. Polycyclic aromatic hydrocarbons in hydromorphic soils of the tropical metropolis Bangkok. Geoderma 1999;91: 297–309.

Wilson NK, McCurdy TR, Chuang JC. Concentrations and phase distributions of nitrated and oxygenated polycyclic aromatic hydrocarbons in ambient air. Atmos Environ 1995;29:2575–84.

Xu HM, Cao JJ, Ho KF, Ding H, Han YM, Wang GH, et al. Lead concentrations in fine particulate matter after the phasing out of leaded gasoline in Xi'an, China. Atmos Environ 2012;46:217–24.

Zhang XY, Cao JJ, Li LM, Arimoto R, Cheng Y, Huebert B, et al. Characterization of atmospheric aerosol over Xi'an in the south margin of the Loess Plateau, China. Atmos Environ 2002;36:4189–99.